Crystalline Cyclic Peptide Nanotubes at Interfaces

Hanna Rapaport,[†] Hui Sun Kim,[‡] Kristian Kjaer,[§] Paul B. Howes,[§] Sidney Cohen,[†] Jens Als-Nielsen,[||] M. Reza Ghadiri,[‡] Leslie Leiserowitz,*[,†] and Meir Lahav[†]

Contribution from the Department of Materials and Interfaces, Weizmann Institute of Science, Rehovot 76100, Israel, Department of Solid State Physics, Risø National Laboratory, DK-4000 Roskilde, Denmark, Niels Bohr Institute, H. C. Ørsted Laboratory, Universitetsparken 5, DK-2100 Copenhagen, Denmark, and Department of Chemistry & Molecular Biology and Skaggs Institute for Chemical Biology, The Scripps Research Institute, La Jolla, California 92037

Received July 9, 1998. Revised Manuscript Received November 19, 1998

Abstract: The assembly, orientation, and structural features of nanoscale tubes composed of cyclic peptides, formed at the air−water interface, were detected by grazing incidence X-ray diffraction (GIXD). The peptide *cyclo*-[(L-Phe-D-*N*-MeAla-)$_4$] (**1**) exhibits two-dimensional crystallinity in which the plane of the peptide ring is parallel to the water interface. The peptide *cyclo*-[(L-Trp-D-Leu)$_3$-L-Ser-D-Leu] (**2**) forms predominantly planar aggregates composed of several tubes, lying with their long axes parallel to the air−water interface. In contrast, the peptide *cyclo*-[(L-Trp-D-Leu)$_4$] (**3**) exhibits a very low tendency to form ordered two-dimensional arrays of nanotubes. Films of peptides **2** and **3** as well as their mixtures with the phospholipid DPPA were transferred onto a solid support and visualized by scanning force microscopy (SFM).

Introduction

Artificially designed channels composed of organic compounds have diverse potential functionalities ranging from catalysis[1] and adsorption[2] to size-selective transporting systems.[3] Cyclic peptides composed of alternating D and L amino acids self-assemble into nanoscalar tubular structures[4] exhibiting potential application for the formation of inorganic nanocluster composites, biologically relevant transmembrane channels, and pore assemblies on solid surfaces generating an ion sensor device.[5] One of the advantages this group of cyclic peptides renders is the versatile surface characteristics the tubular assemblies might possess. Smooth interfaces provide a tunable environment for the generation of controlled layered assemblies of mono- and multilayer molecular thick films.[6]

Here we aim toward elucidation of some of the structural factors that govern the supramolecular organization of the three cyclic peptides **1**−**3** belonging to the class of self-assembling peptide nanotubes. This study was carried out by grazing incidence X-ray diffraction (GIXD) of Langmuir films of the peptides. Films of **2** and **3** were transferred by horizontal deposition onto atomically smooth mica and imaged by scanning force microscopy (SFM). The effect of the phospholipid L-α-phosphatidic acid dipalmitoyl[7] (DPPA) on the aggregation behavior of peptides **2** and **3** was also studied by both GIXD and SFM.

Experimental Section

The cyclic peptides[5] were dissolved in trifluoroacetic acid−chloroform (1:4 volume to volume) to a final concentration of approximately 0.05 mg/mL. L-α-Phosphatidic acid dipalmitoyl was purchased from Sigma.

Surface pressure−area isotherms were measured on water subphases using a KSV minitrough, 240 × 75 mm^2 (KSV Instruments Ltd., Helsinki, Finland).

Grazing Incidence X-ray Diffraction. A detailed description of the GIXD method is given in ref 6b. The experiments were performed at the undulator BW1 beam line on a liquid surface diffractometer at the HASYLAB synchrotron source (Hamburg, Germany). A monochromated X-ray beam was adjusted to strike the liquid surface at an incident angle ($\alpha \approx 0.85\alpha_c$ where α_c is the critical angle for total external reflection) which maximizes surface sensitivity. The dimensions of the footprint of the incoming X-ray beam on the liquid surface were approximately 5 × 50 mm^2. GIXD signals were obtained from two-dimensional (2D) crystallites with an azimuthally random orientation. The scattered intensity was collected by means of a position-sensitive detector (PSD) which intercepted photons over the range $0.0 \le q_z \le 0.9$ Å^{-1}, where $q_z \approx (2\pi/\lambda) \sin \alpha_f$ is the vertical component of the X-ray scattering vector, α_f being the angle between the horizon and the diffracted beam. Measurements were performed by scanning with the PSD along the horizontal scattering vector $q_{xy} \approx 4\pi \sin \theta_{xy}/\lambda$, where $2\theta_{xy}$ is the angle between the incident and diffracted beams projected onto the horizontal plane. These diffraction data are represented in two ways: The grazing incidence diffraction pattern shows the Bragg peak intensity profiles $I(q_{xy})$ obtained by integrating the whole q_z intensity for each q_{xy}. Bragg rod profiles show the scattered intensity $I(q_z)$ resolved in channels along the PSD and integrated over the whole q_{xy} range for a Bragg peak.

The q_{xy} positions of the Bragg peaks yield the lattice repeat distances $d = 2\pi/q_{xy}$, which may be indexed by the two Miller indices h,k to yield the unit cell. The full width at half-maximum (FWHM) of the Bragg peaks in q_{xy} units yields the 2D crystalline coherence length[8] associated with the h,k reflection. The width of the Bragg rod profile along q_z gives a measure of the thickness of the crystalline film[6b] ≈0.9-

[†] Weizmann Institute of Science.
[‡] The Scripps Research Institute.
[§] Risø National Laboratory.
[||] H. C. Ørsted Laboratory.

(1) Abrahams, B. F.; Hoskins, B. F.; Michall, D. M.; Robson, R. *Nature* **1994**, *369*, 272.
(2) Venkataraman, D.; Lee, S.; Zhang, J.; Moore, J. S. *Nature* **1994**, *371*, 591.
(3) Harada, A.; Li, J.; Kamachi, M. *Nature* **1993**, *364*, 516.
(4) Ghadiri, M. R.; Granja, J. R.; Milligan, R. A.; McRee, D. E.; Khazanovich, N. *Nature* **1993**, *366*, 324.
(5) Hartgerink, J. D.; Clarck, T. D.; Ghadiri, M. R. *Chem.—Eur. J.* **1998**, *4*, 1367 and references therein.
(6) (a) Berge, B.; Lenne, P. F.; Renault, A. *Curr. Opin. Colloid Interface Sci.* **1998**, *3*, 321. (b) Als-Nielsen, J.; Jacquemain, D.; Kjaer, K.; Levellier, F.; Lahav, M.; Leiserowitz, L. *Phys. Rep.* **1994**, *246*, 251.
(7) Rapaport, H.; Kuzmenko, I.; Kjaer, K.; Howes, P. B.; Bouwman, W.; Als-Nielsen, J.; Leiserowitz, L.; Lahav, M. *J. Am. Chem. Soc.* **1997**, *119*, 11211.
(8) Guinier, A. *X-ray Diffraction*; Freeman: San Francisco, CA, 1968.

10.1021/ja982420i CCC: $18.00
Published on Web 01/27/1999

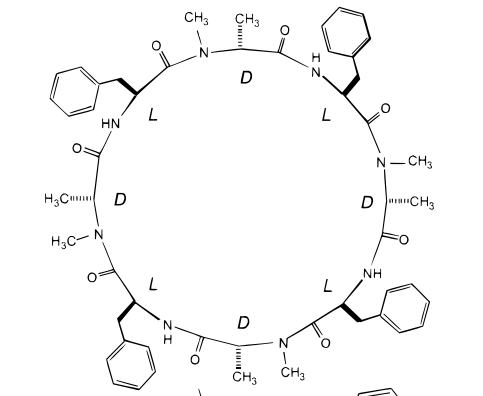

1

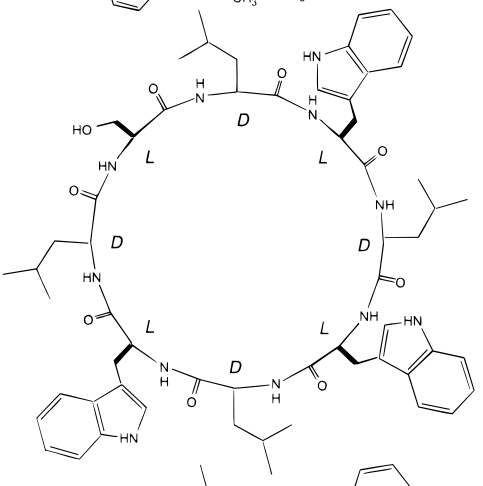

2

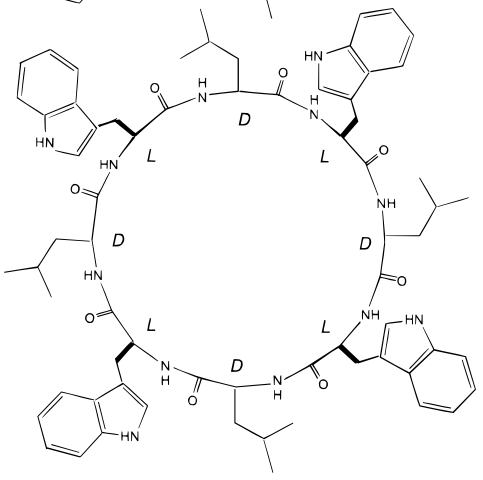

3

$(2\pi)/\Delta q_z$. The intensity at a particular value of q_z in a Bragg rod is determined by the square of the molecular structure factor $|F_{hk}(q_z)|^2$, thus allowing its evaluation according to an atomic model of the molecules. For structure determination of these systems, we used CERIUS[2] molecular simulation computational package.

Scanning Force Microscopy. Freshly cleaved mica pieces were placed on a stainless steel mesh, in the water subphase of a Teflon trough. The cyclic peptide solution (same concentration as for surface pressure−area isotherms measurements) was spread at the air−water interface for a coverage corresponding to 60 Å^2, nominal area per molecule. The subphase was then cooled to 5 °C, the temperature at which the GIXD studies were performed. The water subphase was slowly drained with a motor-driven syringe so that the cyclic peptide film was horizontally deposited onto the mica surface.[9] SFM images were taken with a Topometrix TMX 2010 Discoverer system. Measurements were made using silicon nitride pyramidal tips on cantilevers with spring constants of 0.5 N/m (Park, Sunnyvale, CA), except when indicated as intermittent contact mode, using probes with resonance frequencies between 280 and 310 kHz (Nanosensor, Welzar-Blanenfeld, Germany).

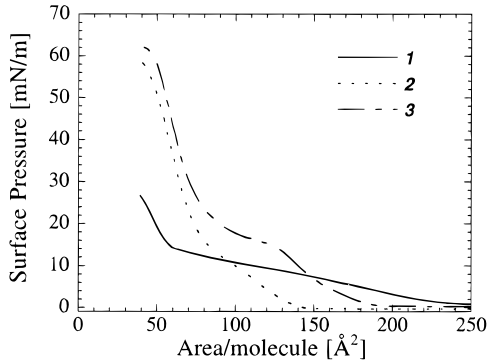

Figure 1. Surface pressure−area isotherms of the cyclic peptides on water measured at 20 °C: **1** (full line); **2** (dotted line); **3** (dash-dotted line). The isotherm of peptide **2** was also measured at 5 °C, generally exhibiting a pattern similar to that at 20 °C, but where the steep increase in pressure starts at ∼70 Å^2, reflecting the stronger tendency of the peptide to aggregate at the lower temperature.

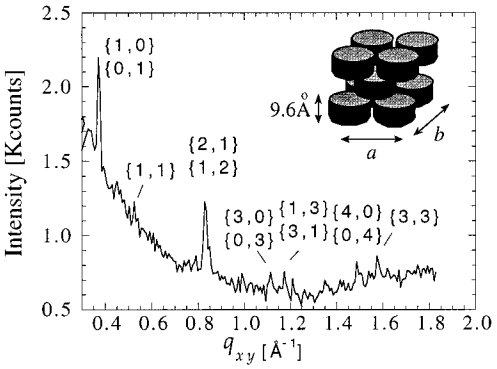

Figure 2. Diffraction pattern of the peptide **1**. The Bragg peaks can be indexed according to a square lattice with $a = b = 16.8$ Å and $\gamma = 90°$. These unit cell dimensions are equal to those of the three-dimensional (3D) crystal $a = b = 16.78$ Å and $c = 22.1$ Å, which is body-centered tetragonal $I422$.[10] This 3D crystal is composed of hydrogen-bonded dimers forming layers parallel to the *ab* plane, in which neighboring layers are offset by $^1/_2 + x$, $^1/_2 + y$, $^1/_2 + z$. We may deduce that the molecular arrangements in the film and the 3D crystal are similar. The full width half-maxima of the Bragg rods yield a film thickness of ∼30 Å. A schematic view of the peptide packing is shown in the inset.

Results

Surface pressure−area isotherms of films of the three cyclic peptides **1**−**3**, each deposited on water surface, were measured (Figure 1); the patterns imply differences in aggregation behavior especially between peptide **1** and the other two peptides. Hysteresis curves of peptide **2** (not shown) indicate that, upon compression of the film at the air−water interface, pronounced and highly irreversible aggregation of the molecules takes place.

A GIXD pattern of the peptide film of *cyclo*-[(L-Phe-D-*N*-MeAla-)$_4$] (**1**) obtained at the air−water interface, at an average area per molecule of 30 Å^2 (Figure 2), exhibits seven Bragg reflections which can be assigned to a square lattice with the unit cell dimensions $a = b = 16.8$ Å and a structure (described in the caption of Figure 2) akin to the body-centered tetragonal[10] structure of the three-dimensional crystalline counterpart. The diffraction pattern indicates that the plane of the cyclic peptide

(9) Majewski, J.; Margulis, L.; Weissbuch, I.; Popovitz-Biro, R.; Arad, T.; Arad, Y.; Lahav, M.; Leiserowitz, L. *Adv. Mater.* **1995**, *7*, 26.

(10) Ghadiri, M. R.; Kobayashi, K.; Granaja, J. R.; Chadha, R. K.; McRee, D. E. *Angew. Chem., Int. Ed. Engl.* **1995**, *34*, 93.

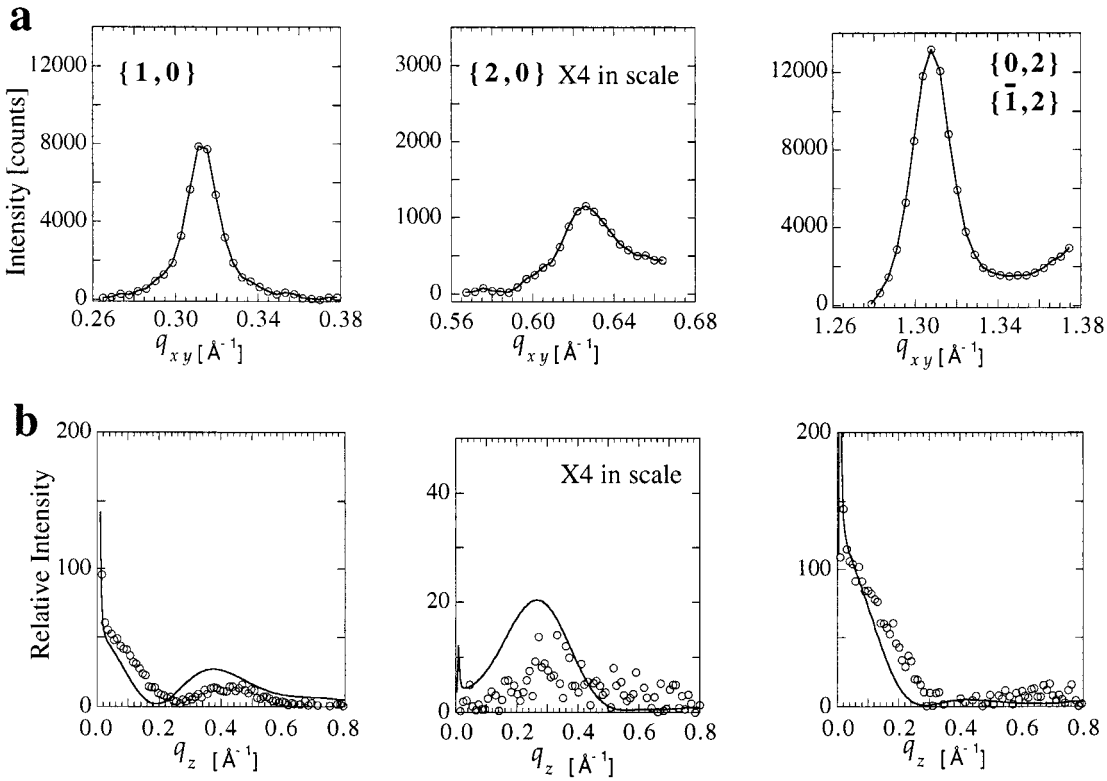

Figure 3. (a) Measured Bragg peaks of peptide **2** at $q_{xy} = 0.31$, 0.62, and at 1.31 Å^{-1}, obtained at a nominal area per molecule of 100 Å^2. (b) Corresponding Bragg rods of peptide **2** (circles). The calculated Bragg rods (full line) were derived by atomic X-ray structure factor analysis using the molecular model shown in Scheme 1b.

Table 1. Results for Peptide **2** and Its Mixtures with DPPA

sample	nominal area per molecule (Å^2)	L_{xy}[a] (Å) at q_{xy} = 0.3 Å^{-1}	L_{xy} (Å) at q_{xy}= 1.3 Å^{-1}
pure peptide[b]	100	400	1150
1:1 [peptide **2**:DPPA], I[c]	66	750	800
1:1 [peptide **2**:DPPA], II[d]	50	250	250
1:5 [peptide **2**:DPPA][e]	30	200	300

[a] L_{xy} is the crystalline lateral coherence length, evaluated by Scherrer's formula from the FWHM of the Bragg peaks. [b] Measured also at a nominal area of 60 Å^2, giving results similar to those at 100 Å^2. [c] Two different experiments for the 1:1 mixture, designated by I and II, are represented. [d] Measured also at a nominal area of 30 Å^2, giving similar results. [e] The two peaks were already observed at a nominal area of 75 Å^2, but their intensities were too weak to be analyzed.

ring is oriented parallel to the water surface. The crystallites detected were ~30 Å thick according to the FWHM of the Bragg rods, implying three layers of cyclic peptide dimers (inset of Figure 2).

GIXD measurements of the film of peptide **2** were performed at a nominal area per molecule of 100 Å^2 and also at 65 Å^2. Both $I(q_{xy})$ scans yielded three Bragg peaks, at q_{xy} values of 0.31, 0.62, and 1.3 Å^{-1} (Figure 3a). The peak at q_{xy} =1.31 Å^{-1} corresponds to a 4.8 Å intersubunit spacing between adjacent stacked cyclic peptides,[4] interlinked by N−H···O bonds, forming a horizontal oriented nanotube which is 1150 Å in coherence length, according to the FWHM of the Bragg peak (Table 1). The peak at $q_{xy} = 0.31$ Å^{-1} and its second-order at $q_{xy} = 0.62$ Å^{-1} correspond to a 19.9 Å spacing which may be assigned to the repeat distance between laterally packed nanotubes. The crystalline coherence length of 400 Å in the direction corresponding to the peak at $q_{xy} = 0.31$ Å^{-1} indicates domains consisting of about 20 nanotubes in lateral registry. The ratio of the coherence length of the peaks at $q_{xy} = 1.31$ Å^{-1} and at 0.31 Å^{-1} (=1150:400 ≈ 2.5:1) may, to a first approximation, be regarded as the aspect ratio of the nanotube crystalline domain. This ratio measured in lattice spacings, (1150/5):(400/20) ≈ 10:1, reflects the strong hydrogen-bond interactions between peptide rings along the nanotube, in comparison to the weak intertube van der Waals contacts.

The three Bragg rods obtained by the GIXD (Figure 3b) were used for the elucidation of the general packing structure of peptide **2**. X-ray structure factor calculations of several proposed atomic models yield Bragg rod profiles which, by comparison with the experimental data, lead to the most probable packing description of the nanotube ordered arrays. In contrast to the case of cyclic peptide **1**, a three-dimensional crystal of peptide **2** has not yet been obtained. The packing characterization described herein relies on structural features common to this family of tubular aggregates.[4] The hydrogen-bond network along the tube links neighboring cyclic peptides spaced 4.8 Å apart, via a 2-fold symmetry.[11] As for the intertube packing, two essentially distinct models were considered. The first model incorporates an arrangement in which nanotubes are packed in a square unit cell with dimensions $a = 20.0$ Å, $b = 9.6$ Å, and $\gamma = 90°$, which implies no offset between neighboring nanotubes, in a direction parallel to the tube axis (Scheme 1a). Such a model yields too strong an intensity of the Bragg rod at $q_{xy} = 1.31$ Å^{-1}, compared with the peak at $q_{xy} = 0.31$ Å^{-1}, for any azimuthal orientation of the tube about its axis, and is thus discarded.

In the second model, the neighboring nanotubes are displaced by a distance of (4.8/2) = 2.4 Å in the direction of the tube axis to permit interleaving between the peripheral groups (as shown in Scheme 1b). The resulting unit cell dimensions are

(11) It is possible to have three different types of dimers dependent on the direction of the 2-fold axis. Nevertheless, the effect of such permutations on the calculated values of the X-ray structure factors are minor and thus discarded.

Scheme 1

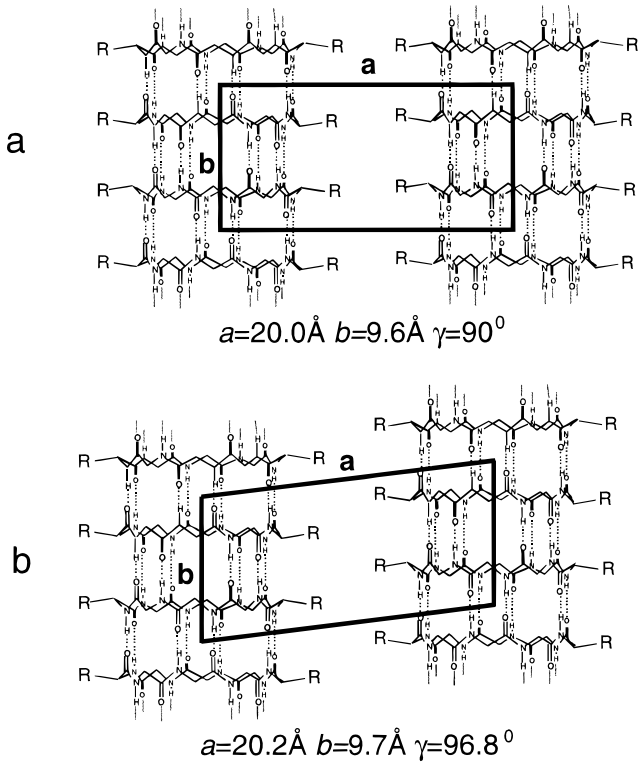

$a = 20.2$ Å, $b = 9.7$ Å, and $\gamma = 96.8°$. This offset motif occurs in the 3D crystal structure of *cyclo*-[(D-Ala-L-Glu-D-Ala-L-Gln)$_2$].[4] The remaining question relates to the azimuthal orientation of the tube on the plane of the water surface.

Several orientations were examined by lattice energy minimization procedures using the CERIUS[2] software package. The best model obtained (Figure 4) is with tryptophan and serine groups lying at opposite sides of the cyclic peptide ring, yielding favorable intermolecular energies, including stacking of tryptophan groups between neighboring tubes. This raftlike monolayer of tubes also gives a reasonable match between the observed and calculated Bragg rod intensity profiles (Figure 3b, full line). The model was not improved further because of the sparseness of the observed data. Given this monolayer arrangement, we may rationalize the observation that an ordered bilayer of nanotubes of peptide **2** is not formed upon compression of the film; such a bilayer would impose poor contacts between tryptophan groups of the adjacent layers. Moreover, on the basis of this model, we may preclude for peptide **3** the formation of an analogous ordered monolayer of nanotubes, which would require unfavorable intertube contacts between the tryptophan moieties. As indeed observed, peptide **3** does not produce observable diffraction signals. These results substantiate the role played by a small and flexible residue such as Ser in forming satisfactory intertube contacts.

The structural effect that the phospholipid DPPA may have on the aggregation behavior of the peptides was studied. Mixtures of peptide **2** with DPPA in peptide:lipid molar ratios of 1:1 and 1:5 gave rise to a diffraction pattern (not shown) which consists of the three Bragg reflections ascribed to the ordered nanotubes and, also, Bragg peaks attributed to ordered phospholipid domains.[12] The crystal coherence lengths associated with the Bragg peaks at $q_{xy} = 0.31$ and 1.31 Å become more equal in the presence of the phospholipid (Table 1). This result suggests a more isotropic shape of the nanotube crystalline domains.

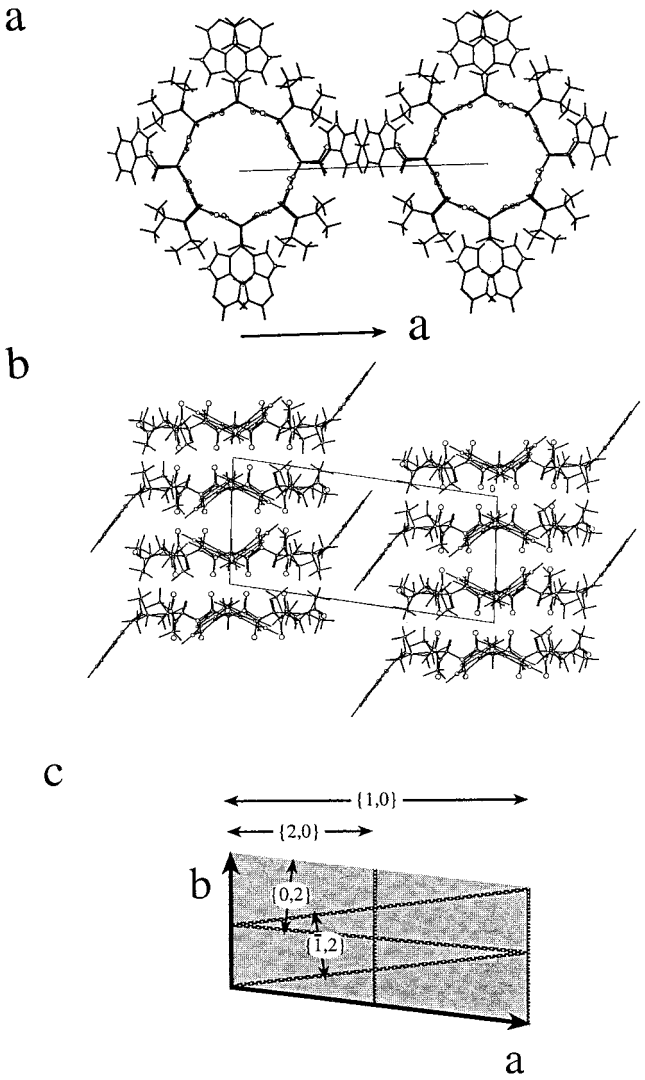

Figure 4. (a) Packing arrangement of the model shown in Scheme 1b, of unit cell dimensions $a = 20.2$ Å, $b = 9.7$ Å, and $\gamma = 96.8°$, viewed along the *b* axis. (b) View of the model along the normal to the air−water interface. (c) Scheme of the model unit cell with lines corresponding to the diffracting planes; *h,k* Miller indices are indicated.

SFM images of films of pure peptide **2** deposited on mica support (Figure 5A) revealed elongated structures ranging in length from ∼400 to ∼1000 Å and in width from ∼100 to ∼250 Å, with a height of ∼18 Å. On the basis of the GIXD data discussed above, we may assume that these structures correspond to bundles of nanotubes oriented with their long axes parallel to the solid support. The lengths of the tubular aggregates detected by SFM are in the same range as the crystal coherence lengths estimated by GIXD.

The deposited film of the equimolar mixture of DPPA and cyclic peptide **2** resulted in the separation of the two components into distinct phases (Figure 5B,C). Lateral force measurements (Figure 5C) emphasized the presence of different domains. In the shear force scan mode, the aggregates of nanotubes oriented with their long axes parallel to the solid support exhibit stronger interactions with the SFM tip (Figure 5C, light gray) than the DPPA islands (Figure 5C, dark gray). These differences may be due both to the inert nature of the phospholipid domains,

(12) The mixtures of the cyclic peptide **2** and DPPA measured by GIXD yielded also a Bragg peak of repeat distance of 4.12 Å attributed to DPPA: Kjaer, K.; Als-Nielsen, J.; Helm, C. A.; Lauhuber, L. A.; Mohwald. *Phys. Rev. Lett.* **1987**, *58*, 2224.

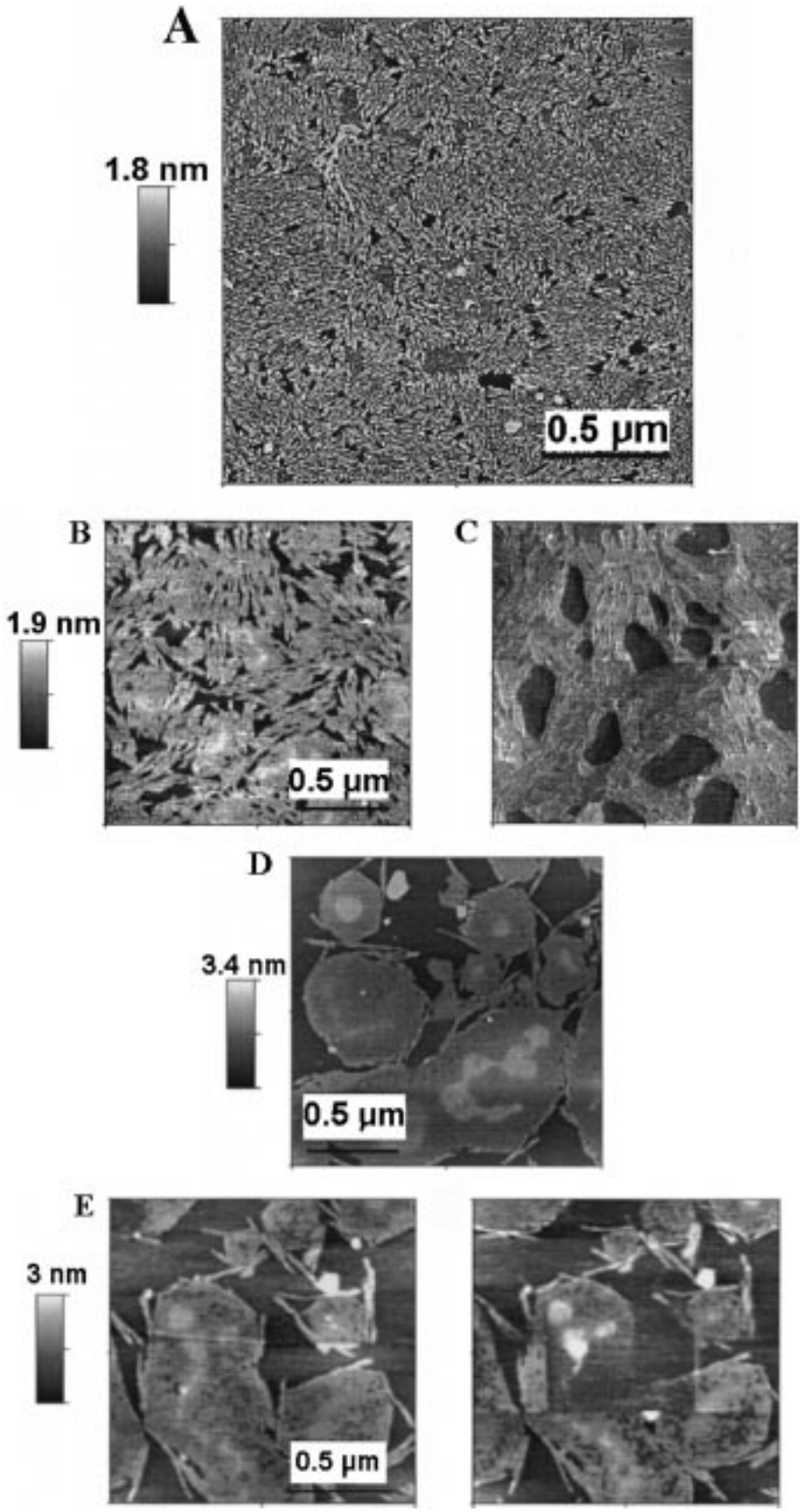

Figure 5. SFM images of films transferred onto mica supports by horizontal deposition. (A) Topography of pure cyclic peptide. Elongated bundles are observed. (B) Topography scan of the 1:1 mixture film. (C) Lateral force image of the same spot shown in (B), demonstrating the differences between the phospholipid (dark gray domains, low friction) and the nanotubes (light gray domains, high friction) oriented parallel to the surface. (D) Topography of the 1:10 film. Phospholipid islands are decorated by elongated bundles of nanotubes. Aggregates embedded within the phospholipids are observed. (E) Topography of a different spot of the 1:10 film. Part of the film (square in shape) was scanned, on purpose, by higher force applied by the SFM tip. The phospholipid was mostly swept away by the tip whereas the embedded aggregates remained almost unaffected.

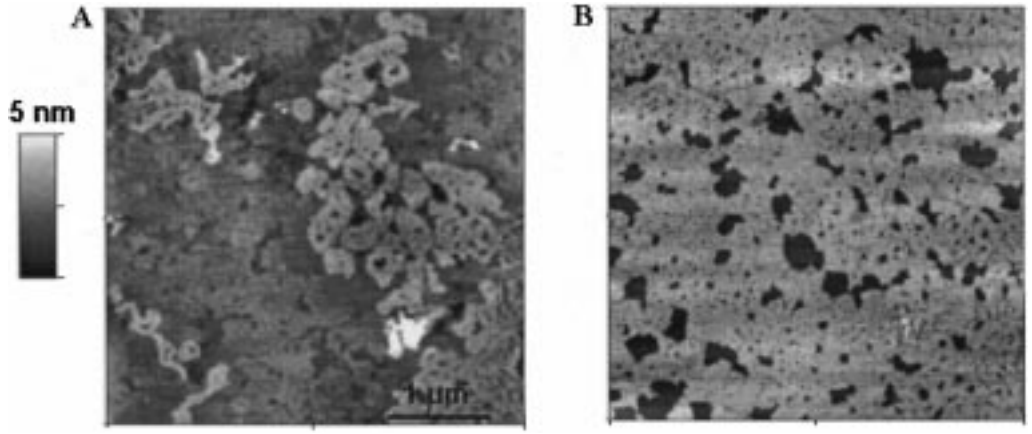

Figure 6. (A) Topography scan of an equimolar mixture of peptide **3** and DPPA deposited at a nominal area per molecule of 60 Å^2. (b) Lateral force image of the same spot shown in (A).

exposing their terminal methyl groups, and to the close packing of the DPPA acyl chains, which decreases the interactions with the SFM tip. The bundles of nanotubes display a tendency to assemble at the rim of the phospholipid domains. Moreover, these structures, which are about 1500 Å in length, appear to be markedly longer than the typical aggregates (400−1000 Å in length as observed by SFM) formed by the pure peptide (cf. Figure 5A). SFM images of the film with a peptide:lipid ratio of 1:10 are shown in Figure 5D,E. The phospholipid forms close-packed sections, some hexagonal-like in shape, indicating intrinsic order of the lipid molecules. The periphery of the lipid domains are decorated with elongated bundles of nanotubes lying parallel to the mica surface. In accordance with lower peptide-to-lipid ratio, the number of these tubular assemblies is lower than it is in the equimolar sample. Aggregates that emerge by ∼10−40 Å above the phospholipid islands (Figure 5D), which were distinguished also by wear experiments (Figure 5E and caption), might be attributed to the peptide.

The deposited films of peptide **3** (not shown) and its mixtures with DPPA, 1:1 (Figure 6) and 1:10 (not shown), were also studied by SFM. The pure peptide forms aggregates less definitive in shape than those of peptide **2**, and elongated bundles were only rarely observed. Similarly, for the films of the 1:1 and 1:10 mixtures, no apparent aggregation of nanotubes was detected. Moreover, no correlation could be made between the topography and lateral force images (Figure 6). Presumably, the domains differentiated by the lateral force correspond to different amorphous mixtures of the two components.

Discussion

The three peptides studied differ in their aggregation behavior. Peptide **1** forms 2D crystallites composed of layers of about three hydrogen-bonded cyclic dimers stacked perpendicular to the plane of the water surface. The GIXD data indicate that peptide **2** forms crystalline monolayers of nanotubes lying parallel to the water surface in raftlike aggregates. The SFM scan displays images of elongated aggregates in keeping with the GIXD data. Peptide **3** does not tend to form ordered arrays of nanotubes according to the GIXD data, as also supported by the SFM measurements. A comparison of the behavior of peptides **1**−**3** pinpoints the importance played by the nature of the peptide groups and their residues in determining the aggregation behavior of the three systems. The rings of peptide **1**, aligned parallel to the water surface, cannot form a continuous nanotube by hydrogen bonds since it exposes *N*-methyl groups at one side of the ring. The peptidic phenyl and methyl substituents on the ring periphery are of a size to permit crystalline close packing between rings within the layer arrangement. Peptide **2**, on the other hand, forms extended nanotubes by virtue of the continuous hydrogen-bonded network. A comparison of molecules **2** and **3** reveals the importance played by even one out of the eight peptide residues on the molecular periphery. The cyclic peptide **3**, with four bulky Trp groups, barely exhibits a tendency, if at all, to form ordered arrays of nanotubes, whereas peptide **2**, with three Trp groups and one Ser, assembles into ordered 2D arrays of nanotubes.

Conclusions

This study highlights primary factors that seem to be responsible for the differences observed in the formation and stabilization of ordered arrays of peptide nanotubes at the air−water interface. We may speculate that the individual cyclic peptides prefer to orient so that the plane of the ring is parallel to the air−water interface, stabilized by the eight potential hydrogen bonds between the ring and the water subphase. To form a 2D array of nanotubes, which will allow the transfer of solute components through the tubes across the film, it is imperative that the nanotubes be oriented with their central axes normal to the interface, as in the case of transmembrane channels,[13] and be of controllable length. Thus, it is important to control the interplay involving the inherently high hydrogen-bond energy of attachment between the cyclic peptide molecules and the relatively weak interactions between the nanotubes. More favorable intertube interactions might be induced by amino acids with side chains that are more flexible and those capable of forming hydrogen bonds. However, this energy gain would still be insufficient to counterbalance the contribution from the hydrogen-bond network within the tubes. This inherent obstacle might potentially be circumvented by using a "tailor-made" additive such as cyclic peptide **1**, which has *N*-methyl groups at only one side of the cyclic molecule, to cap the end of a nanotube.

Acknowledgment. This work was supported by the United States-Israel Binational Science Foundation and by the office of Naval Research (Grant N00014-95-1-1293) and National Institute of Health (Grant GM 52190). We are indebted to HASYLAB at DESY, Hamburg, Germany, for synchrotron beam time at line BW1.

JA982420I

(13) Kim, H. S.; Hartgernik, J. D.; Ghadiri, M. R. *J. Am. Chem. Soc.* **1998**, *120*, 4417.